CHEMISTRY OF MATERIALS
Article

Chem. Mater. **2009,** *21,* 3315–3324 3315
DOI:10.1021/cm900838b

Enhancing the Properties of Ruthenium Dyes by Dendronization

Byeong-Kwan An, Paul L. Burn,* and Paul Meredith*

Centre for Organic Photonics & Electronics, The University of Queensland, Chemistry Building, Queensland, Australia 4072

Received March 25, 2009. Revised Manuscript Received May 6, 2009

A family of dendrimers comprising [*cis*-di(thiocyanato)-({4,4′-dicarboxy}-2,2′-bipyridyl)-(4,4′-divinyl-2,2′-bipyridine)]ruthenium(II) cores, first-generation biphenyl-based dendrons and 2-ethylhexyloxy surface groups have been prepared. The dendrimers differ in the number of surface groups attached to the dendrons. The dendrimers were found to be more thermally stable than the corresponding simple complex, [*cis*-di(thiocyanato)-(bis{4,4′-dicarboxy}-2,2′-bipyridyl)]ruthenium (II) (N3), and to aggregate less in solution. The dendrimers were found to bind to titanium dioxide substrates via the two carboxyl groups on the bipyridyl unit. Importantly, the dendrimers were found to be significantly less susceptible to desorption. N3 desorbed rapidly from the titanium dioxide substrates while the dendrimers were still mostly adsorbed even after a day under the same conditions. The dendrimers all formed efficient devices with the best having an efficiency of 6.3 ± 0.1%, which compares favorably to N3 with an efficiency of 6.9 ± 0.1% in the same device configuration.

Introduction

Since their initial report,[1] ruthenium(II) complexes have proven to be the workhorse dyes for photoelectrochemical cells (PECs).[2] The best of the ruthenium(II) dyes have comprised two bipyridyl ligands and two isothiocyanate coligands.[3] For use in PECs, one of the bipyridyl ligands of the dye has typically had one or more moieties that bind to the inorganic wide band gap semiconductor photoanode, usually titanium dioxide. The titanium dioxide is nanoporous and provides a large surface area for photon harvesting. It also has an electron affinity suitable for separating the exciton formed on the dye. For the ruthenium(II) complexes, there have been many studies on the effect of the structure on each of the steps in the generation of electricity from an absorbed photon including the rates of the different processes and methods for enhancing light absorption.[4] Although it is hard to make exact comparisons between published results because of different cell sizes, measurement set-ups, and statistically relevant data, it is clear that PECs containing ruthenium (II) dyes can reliably give global efficiencies in the range 5−10%. However, in spite of the impressive efficiencies, there have been fewer reports on device failure mechanisms;[5] nor are there very long-lived PECs operating under maximum power.[6] In the development of long lifetime organic light-emitting diodes, it has been found that different failure mechanisms become apparent or come into play as the lifetime of the device increases. In terms of the ruthenium(II) complexes used in PECs, there are potential weak points in the materials that can be addressed even at this early stage, such as thermal, binding, and electrochemical and photochemical (including effects of aggregation) stability.

In the development of OLED materials, it has been found that the dendronisation of small molecule metal complexes can lead to materials with enhanced properties including high thermal stability, control over intermolecular interactions, high photoluminescence quantum yields and efficient solution processed devices.[7] We were therefore interested in determining whether the dendronisation of the ruthenium(II) complexes used in dye-sensitized solar cells could lead to improvement in the

*Corresponding author. E-mail: p.burn2@uq.edu.au (P.L.B.); meredith@physics.uq.edu.au (P.M.).

(1) O'Regan, B.; Grätzel, M. *Nature* **1991**, *353*, 737–740.
(2) (a) Nazeeruddin, M. K.; Zakeeruddin, S. M.; Lagref, J. -J.; Liska, P.; Comte, P.; Barolo, C.; Viscardi, G.; Schenk, K.; Grätzel, M. *Coord. Chem. Rev*. **2004**, *248*, 1317–1328. (b) Polo, A. S.; Itokazu, M. K.; Iha, N. Y. M. *Coord. Chem. Rev*. **2004**, *248*, 1343–1361. (c) Robertson, N. *Angew. Chem., Int. Ed.* **2006**, *45*, 2338–2345. (d) Xie, P.; Guo, F. *Curr. Org. Chem*. **2007**, *11*, 1272–1286.
(3) (a) Nazeeruddin, M. K.; Kay, A.; Rodicio, I.; Humphry-Baker, R.; Mueller, E.; Liska, P.; Vlachopoulos, N.; Grätzel, M. *J. Am. Chem. Soc*. **1993**, *115*, 6382–6390. (b) Nazeeruddin, M. K.; Angelis, F. D.; Fantacci, S.; Selloni, A.; Viscardi, G.; Liska, P.; Ito, S.; Takeru, B.; Grätzel, M. *J. Am. Chem. Soc*. **2005**, *127*, 16835–16847.
(4) (a) Nazeeruddin, M. K.; Grätzel, M. Encyclopedia of Electrochemistry; Wiley: New York, 2003; Vol. 6, pp 407−431. (b) Nelson, J. Encyclopedia of Electrochemistry; Wiley: New York, 2003; Vol. 6, pp 432−474.
(5) (a) Hinsch, A.; Kroon, J. M.; Kern, R.; Uhlendorf, I.; Holzbock, J.; Meyer, A.; Ferber *J. Prog. Photovolt: Res. Appl*. **2001**, *9*, 425–438. (b) Sommeling, P. M.; Späth, M.; Smit, H. J. P.; Bakker, N. J.; Kroon, J. M. *J. Photochem. Photobiol., A* **2004**, *164*, 137–144.
(6) (a) Wang, P.; Zakeeruddin, S. M.; Moser, J. E.; Nazeeruddin, M. K.; Sekiguchi, T.; Grätzel, M. *Nat. Mater*. **2003**, *2*, 402–407. (b) Wang, P.; Klein, C.; Humphry-Baker, R.; Zakeeruddin, S. M.; Grätzel, M. *J. Am. Chem. Soc*. **2005**, *127*, 808–809.
(7) (a) Lo, S.-C.; Burn, P. L. *Chem. Rev*. **2007**, *107*, 1097–1116. (b) Lo, S.-C.; Bera, R. N.; Harding, R. E.; Burn, P. L.; Samuel, I. D. W. *Adv. Funct. Mater*. **2008**, *18*, 3080–3090. (c) Gambino, S.; Stevenson, S. G.; Knights, K. A.; Burn, P. L.; Samuel, I. D. W. *Adv. Funct. Mater*. **2009**, *19*, 317–323.

Published on Web 05/29/2009

materials properties that may in the future lead to efficient and more long-lived devices. In this manuscript we report the synthesis of a family of first generation ruthenium(II) complex cored dendrimers that contain biphenyl-based dendrons and differ in the number of surface groups (Figure 1). We compare the physical and photophysical properties of the dendrimers with N3 and a simple distyryl substituted complex that has essentially the same chromophore as the dendrimers.

Results and Discussion

Synthesis. The first step in the syntheses of the complexes was to form the elaborated bipyridyl ligands. All the ligands were prepared by a Horner−Emmons Wittig reaction between the bipyridyl-bisphosphonate **1** and the requisite "benzaldehyde" using potassium *t*-butoxide as the base (Scheme 1). Under these conditions, the simple distyryl-substituted bipyridyl ligand **3** was formed from **2** in a 93% yield, and the first-generation dendronized ligand **5** with four surface groups was formed in a yield of 92% from the previously reported first-generation benzaldehyde **4**.[8] For the dendronized ligand with eight and twelve surface groups, the first-generation aldehyde-focused dendrons had to be formed first. This was achieved by reaction of the di-[9] and trialkoxy[10] boronic acids with 3,5-dibromobenzaldehyde under Suzuki conditions. The first-generation dendron with four surface groups, **6**, was formed in an 81% yield, whereas that containing six surface groups, **8**, was isolated in a 78% yield. **6** and **8** were then coupled with **1** under the standard conditions to give the dendronized ligands **7** and **9** with eight and twelve surface groups in the excellent yields of 87 and 95%, respectively.

The formation of the ruthenium(II) complexes followed the method reported for the synthesis of N3 derivatives.[11] The procedure involves the sequential substitution of the ligands of $\{RuCl(p\text{-cymene})\}_2$. In the first step, the starting complex was treated with the most sterically hindered bipyridyl ligand for four hours at 80 °C in *N*,*N*-dimethylformamide. The intermediate complex was then reacted with 4,4′-dicarboxy-2,2′-bipyridine for 4 h at around 150−160 °C. Finally, an excess of ammonium isothiocyanate was added and the reaction was then left for a further 4 h at 150 °C. The crude product was isolated as the tetra-*n*-butylammonium salt before being completely transformed back to the acid by treatment with dilute nitric acid. Because of the poor solubility of the compounds in the aqueous acid, we found that it was sometimes necessary to repeat the acidification process. We found that it was possible to follow the progress of the removal of the tetra-*n*-butylammonium unit by ^{1}H NMR. Under these conditions, the distyryl-containing complex **10** and the dendrimers with four **11**, eight **12**, and twelve **13** surface groups were isolated in yields of 72, 63, 54, and 30% respectively. The decrease in yields across the series most probably relates to the increase in steric compression with the more highly substituted bipyridyl ligands. The structures of the materials were consistent with their spectra, and in particular, the observed and calculated isotopic distributions for the molecular weights of the materials were the same, with the mass spectrum of **13** shown in Figure 2 by way of an example.

Physical Properties. We first studied the positive effect of dendronization on the thermal properties of the materials by thermal gravimetric analysis. N3 (Figure 3) and **10** are thermally stable and were found to have a 5% weight loss at 320 and 315 °C, respectively. All the dendrimers were stable to higher temperatures, with **11**, **12**, and **13** (Figure 3) having 5% weight losses at 347, 339, and 351 °C, respectively.

The next step in understanding the enhancement of properties given by the dendritic architecture was the effect on the stability of the dye attachment to the titanium dioxide. All the dyes were adsorbed onto the transparent titanium dioxide and their infrared spectra (ATR mode) collected before and after adsorption. The infrared spectra of the materials before adsorption all show similar features with carbonyl stretches of the carboxylic acids in the range of 1712−1729 cm^{-1} and absorptions due to the isothiocyanates near 2100 cm^{-1}. In the carboxylic acid O−H stretching region there does appear to be a difference between the dendritic and nondendritic materials. For N3 (Figure 4) and **10**, the hydroxyl stretches appear to cover a broader range of wavenumbers, suggesting that there is more hydrogen bonding in the solid state for these materials when compared to the dendritic materials (the infrared spectrum of **12** in shown in Figure 4). Hydrogen bonding can lead to aggregation; the effect of aggregation will be discussed further in the section on the absorption properties of the materials. The fingerprint region of the infrared spectra of N3 and **12** as neat materials and on titanium dioxide are shown in Figure 5. The key difference between the two spectra is that for N3 there is still a carbonyl stretch that is due to the carboxylic acid moieties not bound to the titanium substrate.[12] In contrast, in the spectrum of **12**, there is no carbonyl stretch on the substrate corresponding to a free carboxylic acid, indicating that both carboxyl groups are involved in the binding to the titanium dioxide. The infrared spectrum of N3 bound to titanium dioxide has been studied in detail and it has been shown to coordinate to the titanium dioxide through bidentate or bridging coordination rather than monodentate modes.[13] The absorptions at 1380 and 1620 cm^{-1} have been assigned as the symmetric and asymmetric stretches of the $-CO_2$ groups respectively.

(8) Lo, S.-C.; Richards, G. J.; Markham, J. P. J.; Namdas, E. B.; Sharma, S.; Burn, P. L.; Samuel, I. D. W. *Adv. Funct. Mater.* **2005**, *15*, 1451–1458.
(9) Stewart, D.; Mchattie, G. S.; Imrie, C. T. *J. Mater. Chem.* **1998**, 47–51.
(10) Lee, H.; Kim, D.; Lee, H.-K.; Qiu, W.; Oh, N.-K.; Zin, W.-C.; Kim, K. *Tetrahedron Lett.* **2004**, *45*, 1019–1022.
(11) Klein, C.; Nazeeruddin, M. K.; Censo, D. D.; Liska, P.; Grätzel, M. *Inorg. Chem.* **2004**, *43*, 4216–4226.
(12) Finnie, K. S.; Bartlett, J. R.; Woolfrey, J. L. *Langmuir* **1998**, *14*, 2744–2749.
(13) Argazzi, R.; Bignozzi, C. A.; Heimer, T. A.; Castellano, F. N.; Meyer, G. J. *Inorg. Chem.* **1994**, *33*, 5741–5749.

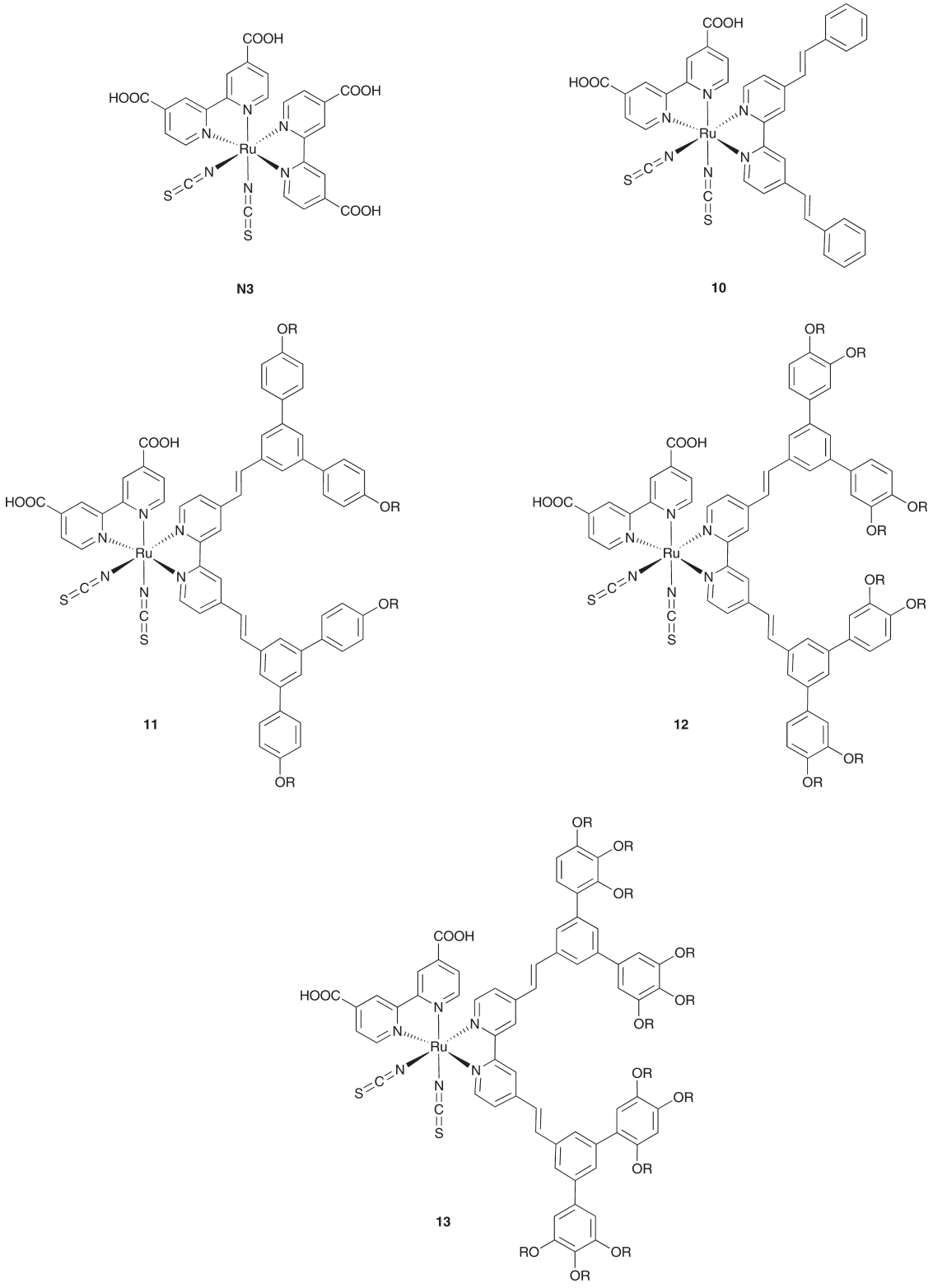

Figure 1. Structures of the materials used in this study. R = 2-ethylhexyl.

Comparison of panels a and b in Figure 5 shows that the fingerprint region of N3 and **12** are very similar, indicating that they are bound to the titanium dioxide in a similar manner.

The nature of the binding of the ruthenium complexes (at best an ester) to the titanium dioxide is a potential weak point for the long-term stability of such dyes in PECs. That is, such bonding will be susceptible to nucleophiles such as water, which would be expected to permeate the device overtime.[2c,4a,14] This is in fact a critical issue, as the actual number of dye molecules

(14) Kroon, J. M.; Bakker, N. J.; Smit, H. J. P.; Liska, P.; Thampi, K. R.; Wang, P.; Zakeeruddin, S. M.; Grätzel, M.; Hinsch, A.; Hore, S.; Würfel, U.; Sastrawan, R.; Durrant, J. R.; Palomares, E.; Pettersson, H.; Gruszecki, T.; Walter, J.; Skupien, K.; Tulloch, G. E. *Prog. Photovolt.: Res. Appl.* **2007**, *15*, 1–18.

Scheme 1 [a]

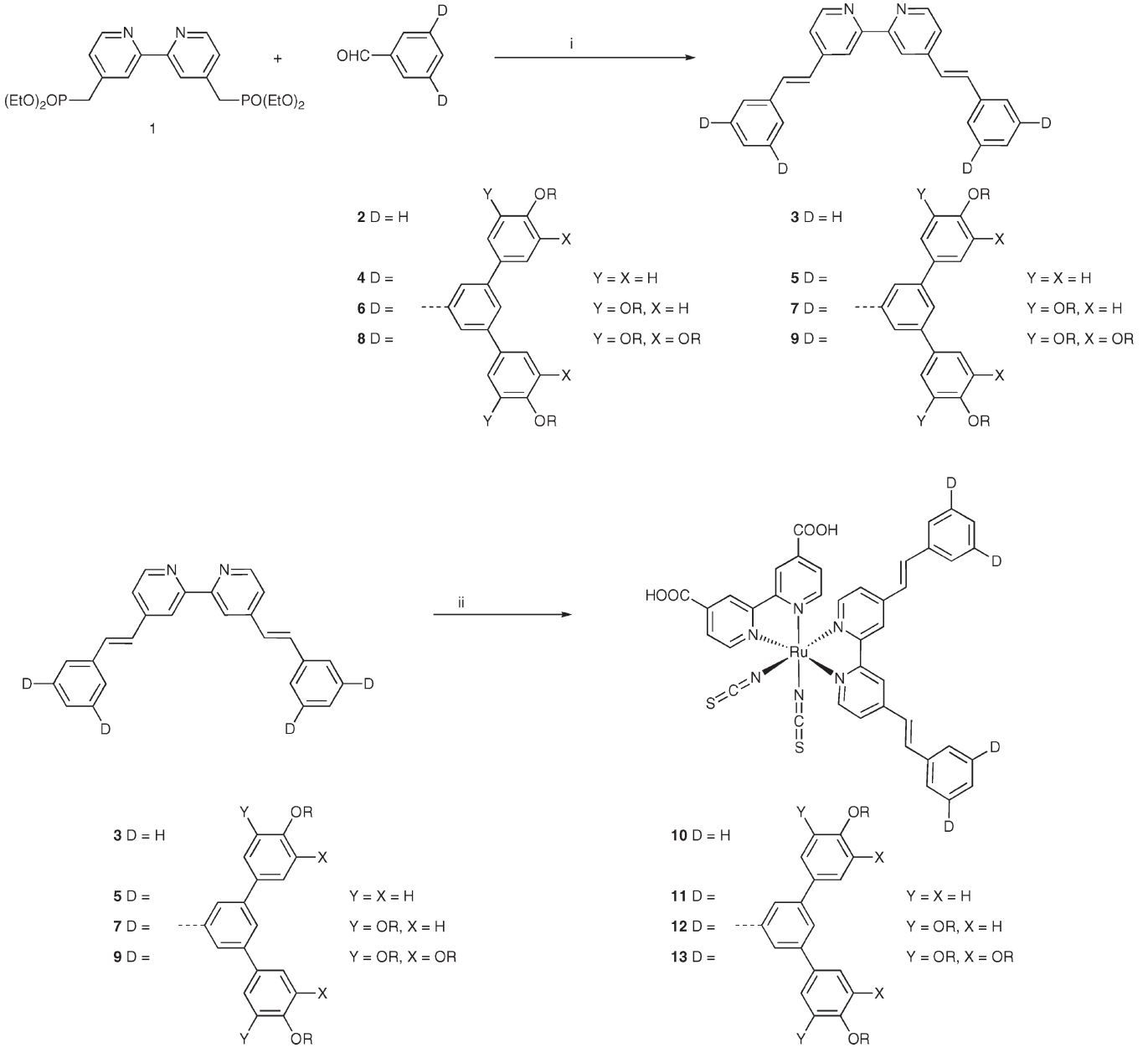

[a] (i) Potassium *t*-butoxide, tetrahydrofuran, r.t.; (ii) {RuCl(*p*-cymene)}$_2$, dendronized ligand, *N*,*N*′-dimethylformamide, 80 °C, N_2, 4 h; then, 2,2′-bipyridine-4,4′-dicarboxylic acid, 150-160 °C, 4 h, dark; then excess of NH_4NCS, 150 °C, 4 h. R represents the 2-ethlylhexyl.

attached to the titanium dioxide is relatively small. To show further the potential advantage of the dendritic materials, we decided to use one of the processes typically used for calculating the amount of dye adsorbed onto the titanium dioxide as an accelerated adsorption stability test. It is well-known that dilute aqueous hydroxide can strip small molecule ruthenium dyes off titanium dioxide;[15] in this accelerated test, we adsorbed the ruthenium dyes onto transparent titanium substrates and then treated them with 0.1 Normal aqueous sodium hydroxide (Figure 6) followed by sequential washes in *N*,*N*-dimethylformamide and then acetonitrile. Although aqueous sodium hydroxide could break the bond between the dyes and the titanium dioxide, it was important to ensure that the desorbed material was removed and hence the latter two washes used solvents in which the materials were soluble. In Figure 6, it can be seen that there is a direct correlation between the structure of the material and its propensity to be desorbed. N3 is almost immediately completely removed from the titanium dioxide (in around one minute). The simple complex **10** with the two styryl groups in place of a pair of carboxylic acid groups was found to be a bit more stable, with 50% being removed in 10 min. In contrast, Figure 6 shows that the dendrimers are very much more stable with all the materials having more than 60% of the dye still adsorbed even

(15) Chen, K.-S.; Liu, W.-H.; Wang, Y.-H.; Lai, C.-H.; Chou, P.-T.; Lee, G.-H.; Chen, K.; Chen, H.-Y.; Chi, Y.; Tung, F.-C. *Adv. Funct. Mater.* **2007**, *17*, 2964−2974.

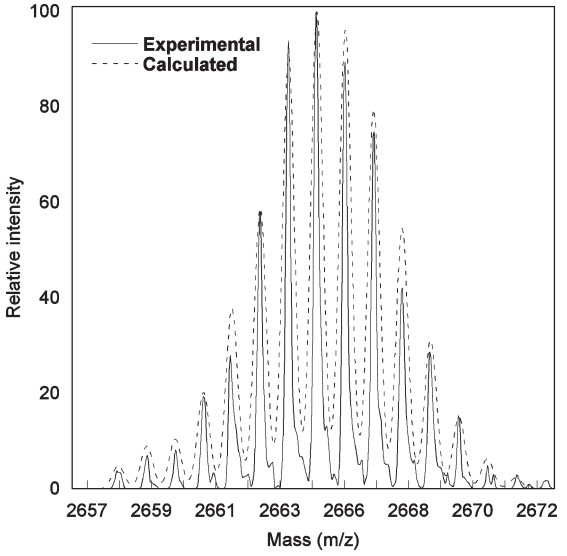

Figure 2. MALDI-TOF mass spectrum of **13**.

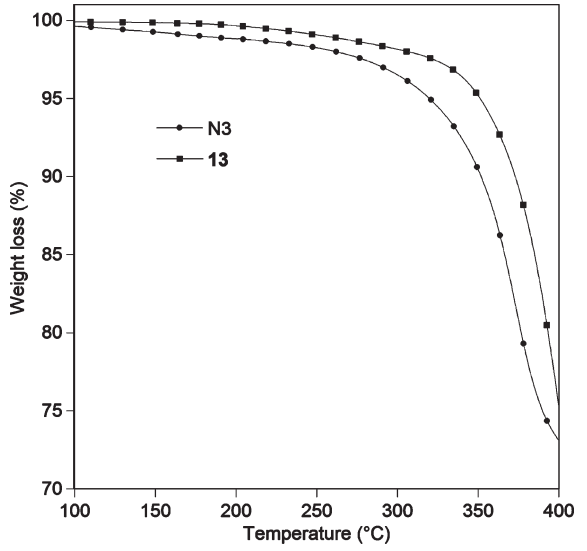

Figure 3. Thermal gravimetric analysis graphs of N3 and **13** showing the enhanced thermal stability of the dendrimer.

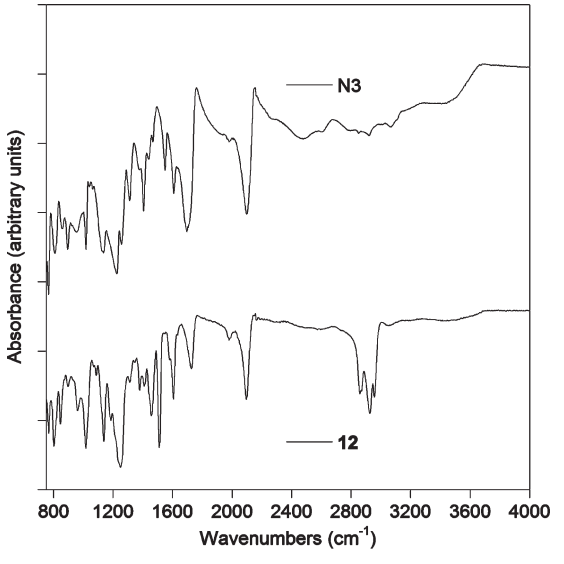

Figure 4. Infrared spectra of neat N3 and **12**.

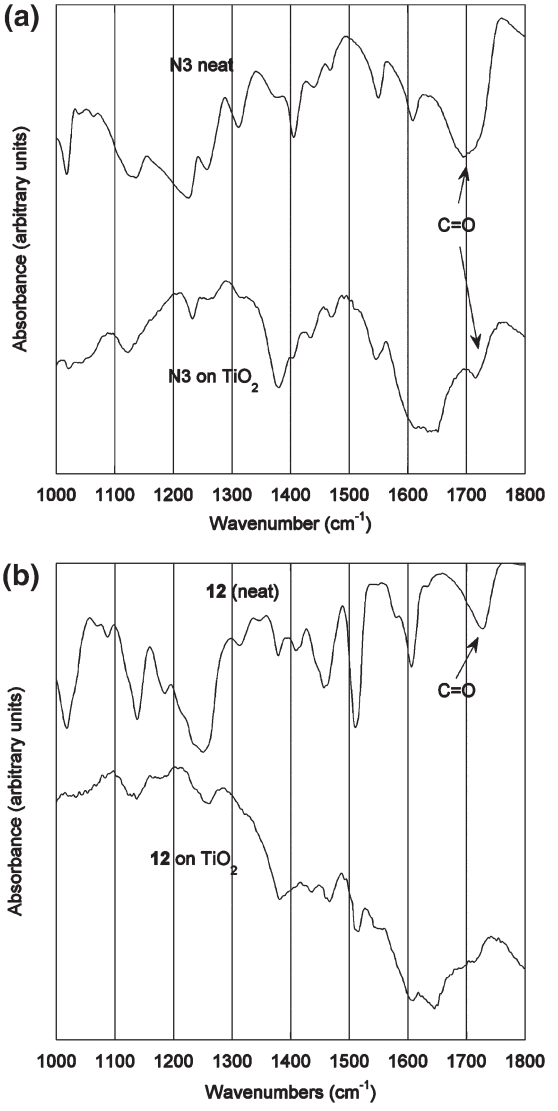

Figure 5. Infrared fingerprint region of (a) N3 and (b) **12** as neat materials and attached to a titanium dioxide film.

after 24 h. The greater stability of the dendritic dyes must be due to the inability of the aqueous hydroxide to penetrate to the titanium dioxide surface to disrupt the binding of the dye. The inability of the nucleophiles to penetrate to the binding sites can be easily understood from the fact that the surface groups of the dendrimers provide a lipophilic "shield" for the active group. The effect of lipophilicity is illustrated in Figure 7, which shows the wetting of N3, **10**, and **11** adsorbed onto titanium dioxide. It can clearly be seen that the contact angle for a water droplet increases from N3 to **10** to **11** (16, 55.3, and 137.8°, respectively) and this follows the same trend observed in the accelerated desorption test, with **11** being the most stable of the three materials.

Photophysical and Device Properties. The recent design strategy for many of the newest ruthenium dyes is to have only one of the bipyridyl ligands with the two carboxylic acid units, and the other having extended conjugated "chromophores" attached.[2] The latter ligands have been designed to red-shift and maximize the absorption at longer wavelengths. It is well-known in the OLED field

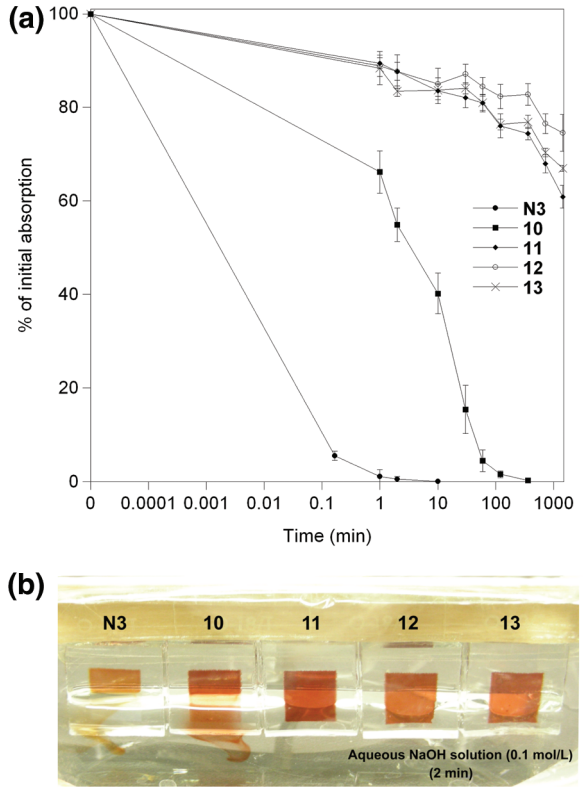

Figure 6. (a) Desorption measurements of the dyes. The *x*-axis is plotted on a logarithmic scale to highlight the different rates of desorption. (b) Photos of dye-adsorbed transparent titanium oxide substrates immersed in 0.1 M aqueous NaOH after 2 min show the rapid desorption of N3 and the stability of the dendrimers.

that close interaction of chromophores can lead to the quenching of the luminescence. This is of the same importance for PEC cells because interactions of the excited states can lead to their quenching before the excited electron is transferred to the titanium dioxide. During the course of this work, we were surprised to discover that the long wavelength absorption spectrum of N3 was concentration dependent (see Figure 8a), even at the very low concentrations used. It was found that the wavelength of the absorption red-shifted by almost 30 nm over concentrations ranging from 0.5×10^{-5} M to 10×10^{-5} M. The most likely cause for the red shift is aggregation of the N3 molecules, which occurs even at these low dilutions. In contrast, the dendrimers showed much less concentration dependence (Figure 8b shows the spectra for dendrimer **13** over the same concentration range). The dendritic nature of **13** means that the ruthenium(II) complex at the focus is less likely to aggregate because of steric hindrance, which lends further credence to the change of absorption for N3 being due to aggregation. A further interesting feature of the spectra is that the there is

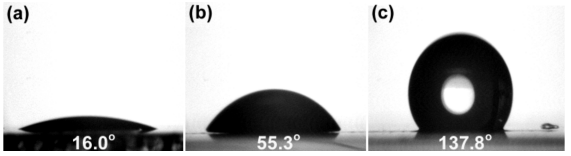

Figure 7. Contact angle for water on (a) N3, (b) **10**, and (c) **11** adsorbed onto titanium dioxide.

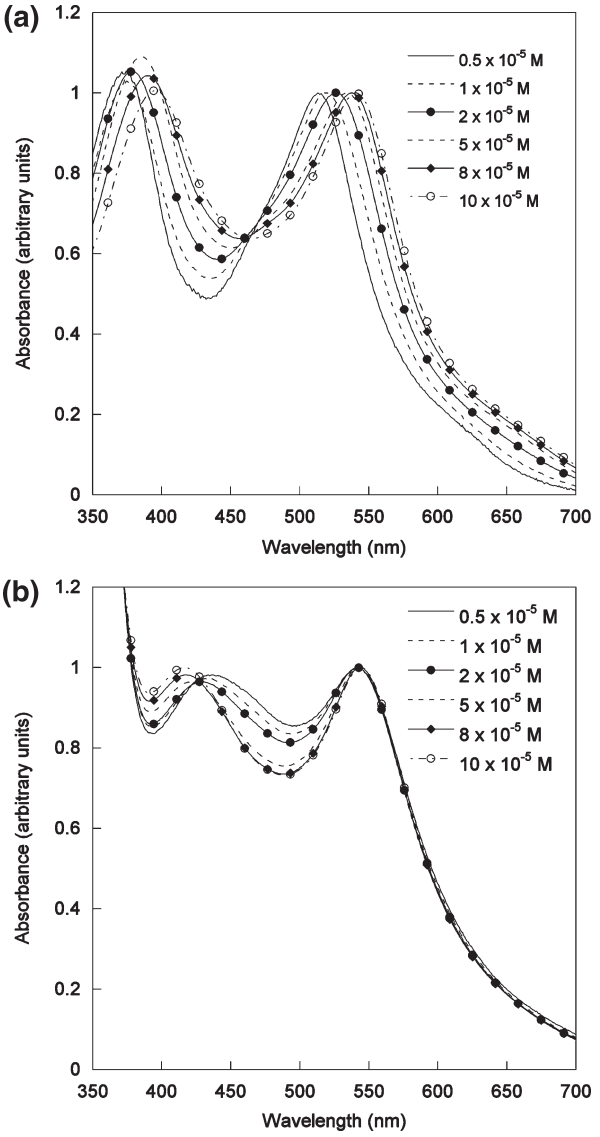

Figure 8. UV−visible absorption spectra of (a) N3 and (b) **12** at different concentrations in *N*,*N*′-dimethylformamide.

not a strong red shift in the long wavelength absorption with the attachment of the "stilbenyl units". In fact, a survey of the ruthenium(II) complexes of this type with "extended" conjugated ligands shows that there is no significant red shift in the long wavelength absorption.[16] Our results suggest that any shift is probably due to the level of aggregation of the complex, which will of course be dependent on the concentration and solvent used to record the spectrum.

DSSCs containing the active dyes were prepared and their performance measured under AM1.5 conditions at ~100 mW/cm^2 (note: the exact power density was

(16) (a) Jang, S.-R.; Lee, C.; Choi, H.; Ko, J. J.; Lee, J.; Vittal, R.; Kim, K.-J. *Chem. Mater.* **2006**, *18*, 5604–5608. (b) Chen, C.-Y.; Wu, S.-J.; Wu, C.-G.; Chen, J.-G.; Ho, K.-C. *Angew. Chem. Int. Ed* **2006**, *45*, 5822–5825. (c) Jiang, K.-J.; Masaki, A.; Xia, J.-B.; Noda, S.; Yanagida, S. *Chem. Commun.* **2006**, 2460–2462. (d) Chen, C.-Y.; Wu, S.-J.; Li, J. −Y.; Wu, C.-G.; Chen, J.-G.; Ho, K.-C. *Adv. Mater.* **2007**, *19*, 3888–3891. (e) Jiang, K.-J.; Xia, J.-B.; Masaki, N.; Noda, S.; Yanagida, S. *Inorg. Chim. Acta* **2008**, *361*, 783–785.

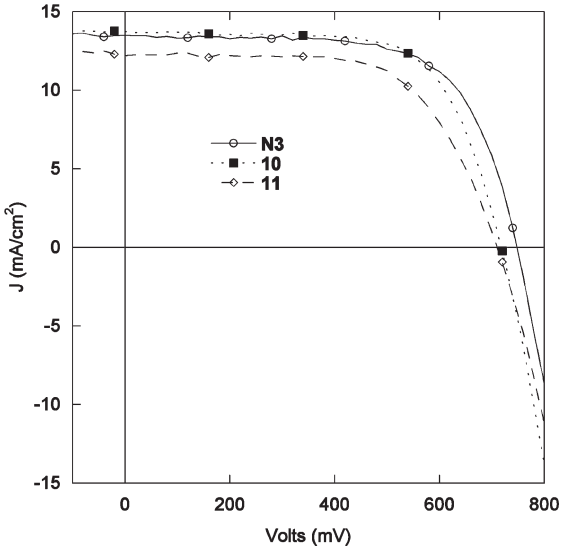

Figure 9. $J-V$ characteristics of DSSCs containing N3, **10**, and **11**.

measured using a broadband thermopile detector and the value was used for the efficiency calculations). The DSSCs comprised titanium dioxide (that had been pretreated with titanium tetrachloride followed by thermal treatment at ~450 °C for 30 min) with an active area on the order of 0.20 cm^2, the adsorbed dye (from 3×10^{-4} M solutions), an electrolyte solution (0.6 M 1-*n*-butyl-3-methylimidiazole iodide, 0.03 M iodide, 0.1 M guanidinium thiocyanate, and 0.5 M *t*-butylpyridine in a 15/85 (v/v) mixture of valeronitrile and acetonitrile), and a platinum on fluorine tin oxide counter electrode. All devices using the new materials showed good efficiencies with the $J-V$ characteristics for N3, **10**, and **11** shown in Figure 9. The efficiencies (averaged over five devices) of N3, **10**, **11**, **12**, and **13** were 6.94 ± 0.12%, 7.19 ± 0.11%, 6.32 ± 0.13%, 5.26 ± 0.08%, and 3.69 ± 0.19% respectively. There are two important points to note from these device results. First, **10** gives a better device performance than N3, and second, the improvement in adsorption stability does not necessarily come at a large cost in terms of device efficiency, with **10** having a performance only a little less than N3.

Conclusion

We have developed a new family of dendrimers with ruthenium(II) complex cores. The dendrimers have first-generation biphenyl-based dendrons and differing numbers of surface groups. The yields of the dendrimers were all good, even for the most sterically encumbered material that had six surface groups per dendron. The dendrimers were found to aggregate less than their small molecule counterparts, thus controlling intermolecular interactions that can lead to the quenching of the excited state when deposited onto a substrate. Most importantly, in terms of the physical properties required for long-term device stability, the dendrimers showed superior thermal properties and less propensity to dye desorption. The dendrimers can all be used in efficient dye-sensitized solar cells.

Experimental Section

General Methods. All commercial reagents were used as received unless otherwise noted. Tetrahydrofuran was distilled from sodium and benzophenone under a nitrogen atmosphere before use. Deactivated silica was formed by adding triethylamine to the silica/solvent slurry before loading onto the column. After the column was packed, it was washed through with the solvent mixture in which the sample was loaded. ^1H and ^{13}C NMR spectra were recorded using a 300 or 400 MHz Bruker spectrometer, in deuterated chloroform or dichloromethane solution; spH = surface phenyl H, bipyH = bipyridyl H, G1-bpH = first-generation branch phenyl H, vinylH = vinyl H. Coupling constants are quoted to the nearest 0.5 Hz. Microanalyses were carried out in the Microanalysis Laboratory of the School of Chemistry and Molecular Biosciences, The University of Queensland. UV−visible absorption measurements were recorded with a Cary Varian 5000 UV−vis−NIR spectrophotometer. Infrared spectra were recorded on a Perkin-Elmer Spectrum 100 ATR-FT-IR spectrometer. Melting points were measured in a glass capillary on a BUCHI Melting Point B-545 and are uncorrected. Thermal gravimetric analysis (TGA) was carried out on a Perkin-Elmer STA6000. Mass spectra were recorded on an Applied Biosystems Voyager matrix-assisted laser desorption/ionization time-of-flight (MALDI-TOF) from 2-[(2-*E*)-3-(4-*tert*-butylphenyl)-2-methylprop-2-enylidene]malononitrile (DCTB) in positive reflection mode at the EPSRC National Mass Spectrometry Centre, Swansea, UK. The transparent titanium dioxide substrates were obtained from DyeSol. The contact angle measurement of a water droplet on the dye adsorbed onto titanium dioxide substrates was carried out by using a Tracker tensiometer (I. T. Concept, France).

4,4′-Bis[(E)-(3,5-bis{4-[2-ethylhexyloxy]phenyl}styryl)-2,2′-bipyridine ***5***. Potassium *tert*-butoxide (0.62 g, 5.5 mmol) was added to a solution of **1** (1.00 g, 2.2 mmol) and 3,5-bis[4-(2-ethylhexyloxy)phenyl]benzaldehyde **4**[8] (2.53 g, 4.9 mmol) in tetrahydrofuran (30 mL). The reaction mixture was stirred for 3 h at room temperature under nitrogen. Water (20 mL) was added and the tetrahydrofuran was removed. The aqueous residue was extracted with dichloromethane (2 × 200 mL). The collected organic layer was washed with brine (100 mL) and water (2 × 200 mL), dried over magnesium sulfate, and filtered; the solvent was removed. The residue was purified by column chromatography over silica (deactivated) using an ethyl acetate:petroleum ether (40−60) mixture (1:3) as eluent to give **5** (2.36 g, 92%). Anal. Calcd for $C_{82}H_{100}N_2O_4$: C, 83.6; H, 8.6; N, 2.4. Found: C, 83.6; H, 8.6; N, 2.4. λ_{max}(tetrahydrofuran) 284 [log ε (dm^3 mol^{-1} cm^{-1}) (5.07)], 324 (4.87), 336sh (4.79). ν_{max} 956 (*trans* C=C−H out of plane bend). δ_H (400 MHz, $CDCl_3$) 8.71 (2 H, d, J = 5, bipyH), 8.62 (2 H, bs, biyH), 7.69 (6 H, s, G1-bpH), 7.64−7.50 (10 H, m, spH and vinylH), 7.44 (2 H, dd, J = 1.5, J = 5, bipyH), 7.27 (2 H, d, J = 16.5, vinylH), 7.04 (8 H, 1/2AA'BB', spH), 3.92 (8 H, m, OCH_2), 1.80−1.70 (4 H, m, CH), 1.60−1.30 (32 H, m, CH_2), 0.99−0.92 (24 H, m, CH_3). δ_C (100.6 MHz, $CDCl_3$) 159.2, 156.4, 149.5, 145.6, 141.9, 137.0, 133.3, 133.0, 128.1, 126.5, 125.7, 123.7, 121.1, 118.2, 114.8, 70.5, 39.4, 30.5, 29.1, 23.8, 23.1, 14.1, 11.1. m/z (ES) Anal. Calcd. for $C_{82}H_{100}N_2O_4$: 1177.7. Found: 1177.8.

3,5-Bis[3,4-bis(4-{2-ethylhexyloxy}phenyl)]benzaldehyde ***6***. A mixture of 3,5-dibromobenzaldehyde (1.59 g, 6.0 mmol), 3,4-bis(2-ethylhexyloxy)phenylboronic acid[9] (5.00 g, 13.2 mmol), tetrakis(triphenylphosphine)palladium(0) (0.09 g, 0.08 mmol), aqueous potassium carbonate (2 M, 15 mL), and tetrahydrofuran (30 mL) was refluxed for 14 h under the nitrogen. After the

solvent was removed, diethyl ether (300 mL) was added and the organic layer was washed with water (3 × 100 mL). The organic layer was dried over anhydrous magnesium sulfate and filtered, and the solvent was removed. The residue was purified by column chromatography over silica using an ethyl acetate: light petroleum (40−60) mixture (1:10) as eluent to give **6** (3.73, 81%). Anal. Calcd for $C_{51}H_{78}O_5$: C, 79.4; H, 10.2. Found: C, 79.6; H, 10.2. λ_{max}(tetrahydrofuran) 344 [log ε (dm^3 mol^{-1} cm^{-1}) (3.43)], 295 (4.26), 278 (4.38). ν_{max} 1700 cm^{-1}. δ_H (400 MHz, $CDCl_3$) 10.15 (1 H, s, CHO), 7.98 (3 H, m, G1-bpH), 7.20 (2 H, dd, J = 2, J = 8.5, spH), 7.17 (2 H, d, J = 2, spH), 6.99 (2 H, d, J = 8.5, spH), 3.95 (8 H, m, OCH_2), 1.85−1.75 (4 H, m, CH), 1.63−1.28 (32 H, m, CH_2), 0.98−0.89 (24 H, m, CH_3). m/z (ES) Anal. Calcd. for $C_{51}H_{78}O_5$: 771.1. Found: 793.6 (M^+ + Na).

4,4′-Bis[(E)-(3,5-bis{3,4-bis[2-ethylhexyloxy]phenyl}styryl)-2,2′-bipyridine **7**. Potassium *tert*-butoxide (0.33 g, 2.9 mmol) was added to a solution of **1** (0.53 g, 1.2 mmol) and **6** (2.00 g, 2.6 mmol) in tetrahydrofuran (30 mL). The reaction mixture was stirred for 3 h at room temperature under nitrogen. Water (10 mL) was added and the tetrahydrofuran was removed. The aqueous residue was extracted with dichloromethane (2 × 200 mL). The combined organic layers were washed with brine (100 mL) and water (2 × 200 mL), dried over magnesium sulfate, and filtered; the solvent was removed. The residue was purified by column chromatography over silica (deactivated) using an ethyl acetate:petroleum ether (40−60) mixture (1:10) as eluent to give **7** (1.70 g, 87%). Anal. Calcd for $C_{114}H_{164}N_2O_8$: C, 81.0; H, 9.8; N, 1.7. Found: C, 80.8; H, 9.7; N, 1.5. λ_{max}(tetrahydrofuran) 302 [log ε (dm^3 mol^{-1} cm^{-1}) (5.00)], 336sh (4.77). ν_{max} 958 (*trans* C═C−H out of plane bend). δ_H (400 MHz, $CDCl_3$) 8.72 (2 H, d, J = 5, bipyH), 8.64 (2 H, bs, bipyH), 7.68 (6 H, m, G1-bpH), 7.62 (2 H, d, J = 16.5, vinylH), 7.46 (2 H, dd, J = 1.5, J = 5, bipyH), 7.28 (2 H, d, J = 16.5, vinylH), 7.22−7.18 (8 H, m, spH), 7.01 (4 H, d, J = 8, spH), 4.02−3.91 (16 H, m, OCH_2), 1.86−1.77 (8 H, m, CH), 1.63−1.30 (64 H, m, CH_2), 0.99−0.90 (48 H, m, CH_3). δ_C (100.6 MHz, $CDCl_3$) 156.5, 149.8, 149.6, 149.5, 145.8, 142.4, 137.0, 133.8, 133.5, 126.5, 126.2, 124.1, 121.3, 119.6, 118.2, 113.7, 112.8, 71.8, 71.7, 39.7, 39.6, 30.6, 29.2, 29.1, 23.9, 23.1, 14.1, 11.23, 11.17. m/z [MALDI-TOF] Anal. Calcd for $C_{114}H_{164}N_2O_8$: 1690.5. Found: 1690.2.

3,5-Bis[3,4,5-tris(4-{2-ethylhexyloxy}phenyl)]benzaldehyde ***8***. A mixture of 3,5-dibromobenzaldehyde (0.95 g, 3.6 mmol), 3,4,5-tris(2-ethylhexyloxy)phenylboronic acid[10] (4.0 g, 7.9 mmol), tetrakis(triphenylphosphine)palladium(0) (0.05 g, 0.05 mmol), aqueous potassium carbonate (2 M, 15 mL), and tetrahydrofuran (30 mL) was refluxed for 14 h under nitrogen. After the solvent was removed, diethyl ether (300 mL) was added and the organic layer was washed with water (2 × 100 mL). The organic layer was dried over anhydrous magnesium sulfate and filtered, and the solvent was removed. The residue was purified by column chromatography over silica using an ethyl acetate:light petroleum (40−60) mixture (1:20) as eluent to give **8** (2.86 g, 78%). Anal. Calcd for $C_{67}H_{110}O_7$: C, 78.3; H, 11.0. Found: C, 78.4; H, 10.65. λ_{max}(tetrahydrofuran) 340 [logε/$dm^3mol^{-1}cm^{-1}$ (3.54)], 277 (3.50). δ_H (400 MHz, $CDCl_3$) δ (ppm) 10.16 (1 H, s, CHO), 7.99 (2 H d, J = 1.5, G1-bpH), 7.95 (1 H, dd, J = 1.5, J = 1.5, G1-bpH), 6.81 (4 H, s, spH), 3.96−3.86 (12 H, m, OCH_2), 1.84−1.71 (6 H, m, CH), 1.61−1.29 (48 H, m, CH_2), 0.98−0.89 (486 H, m, CH_3). m/z (ES) Anal. Calcd for $C_{67}H_{110}O_7$: 1027.6. Found: 1049.8 (M^+ + Na).

4,4′-Bis[(E)-(3,5-bis{3,4,5-tris[2-ethylhexyloxy]phenyl}styryl)-2,2′-bipyridine ***9***. Potassium *tert*-butoxide (0.33 g, 2.9 mmol) was added to a solution of **1** (0.54 g, 1.2 mmol) and **9** (2.70 g, 2.6 mmol) in tetrahydrofuran (30 mL). The reaction mixture was stirred for 3 h at room temperature under nitrogen. Water (10 mL) was added and the tetrahydrofuran was removed. The aqueous residue was extracted with ethylacetate (3 × 100 mL). The combined organic layers were washed with brine (100 mL) and water (2 × 200 mL), dried over magnesium sulfate, and filtered; the solvent was removed. The residue was purified by column chromatography over silica (deactivated) using an ethyl acetate:light petroleum (40−60) mixture as eluent (1:10) to give **9** (2.45 g, 95%). Anal. Calcd for $C_{146}H_{228}N_2O_{12}$: C, 79.6; H, 10.4; N, 1.3. Found: C, 79.7; H, 10.6; N, 1.3. λ_{max}(tetrahydrofuran) 288 [log ε (dm^3 mol^{-1} cm^{-1}) (5.00)], 324 (4.89), 336sh (4.79). ν_{max} 959 (*trans* C═C−H out of plane bend). δ_H (400 MHz, $CDCl_3$) 8.71 (2 H, d, J = 5, bipyH), 8.65 (2 H, bs, bipyH), 7.69 (4 H, bs, G1-bpH), 7.67−7.60 (4 H, m, G1-bpH and vinylH), 7.29 (2 H, d, J = 16, vinyH), 6.82 (8 H, s, spH), 3.99−3.87 (24 H, m, OCH_2), 1.85−1.72 (12 H, m, CH), 1.67−1.28 (96 H, m, CH_2), 0.99−0.89 (72 H, m, CH_3). m/z (ES) Anal. Calcd for $C_{146}H_{228}N_2O_{12}$: 2203.4. Found: 2203.6.

[cis-Di(thiocyanato)-({4,4′-dicarboxy}-2,2′-bipyridyl)-(4,4′-bis-{(E)-2-phenylethenyl}-2,2′-bipyridine)]ruthenium(II) ***10***. {RuCl(*p*-cymene)}$_2$ (150 mg, 0.25 mmol) and **3** (177 mg, 0.49 mmol) were dissolved in distilled *N*,*N*′-dimethylformamide (50 mL). The reaction mixture was heated at 80 °C under nitrogen for 4 h and then 2,2′-bipyridine-4,4′-dicarboxylic acid[17] (120 mg, 0.49 mmol) was added; the reaction mixture was heated at 150−160 °C for another 4 h in the dark to avoid isomerization. An excess of ammonium isothiocyanate (930 mg, 12.25 mmol) was added to the mixture, which was heated at 150 °C for a further 4 h. The reaction mixture was cooled to room temperature and the solvent was removed. Water (20 mL) was added and the insoluble solid was collected by filtration and washed with distilled water (2 × 100 mL). The crude complex was dissolved in a solution of tetra-*n*-butylammonium hydroxide in methanol (5 mL). The concentrated solution was purified by column chromatography using Sephadex LH-20 with methanol as eluent. The main band was collected and solution concentrated. Addition of nitric acid (0.1 M, 10 mL) caused a precipitate to form, which was filtered off. The residue was washed with distilled water and then dried to give **10** as a black solid (290 mg, 72%). Mp > 335 °C. Anal. Calcd for $C_{40}H_{28}N_6O_4RuS_2$: C, 58.5; H, 3.4; N, 10.2. Found: C, 58.4; H, 3.5; N, 10.2. λ_{max}(*N*,*N*′-dimethylformamide) 542 [log ε (dm^3 mol^{-1} cm^{-1}) (4.24)], 416 (4.23), 343sh (4.61). ν_{max} 3500 (br) (−OH), 2093 (−CN), 1712 (-C═O) cm^{-1}. δ_H (500 MHz, DMSO-d, at 373K) 9.53 (1 H, d, J = 5.5, bipyH), 9.22 (1 H, d, J = 5.5, bipyH), 9.04 (1 H, bs, bipyH), 8.88 (2 H, bs, bipyH), 8.72 (1 H, bs, bipyH), 8.24 (1 H, d, J = 5.5, bipyH), 8.04 (1 H, d, J = 5.5, bipyH), 7.96−7.85 (2 H, m, bipyH &/or vinylH &/or phH), 7.80 (2 H, m, bipyH &/or vinylH &/or phH), 7.67 (4 H, m, bipyH &/or vinylH &/or phH), 7.59−7.19 (10 H, m, bipyH &/or vinylH &/or phH). m/z (ES) Anal. Calcd for $C_{40}H_{28}N_6O_4RuS_2$: 816.07 (14%), 817.1 (7%), 818.1 (8%), 819.1 (32%), 820.1 (45%), 821.1 (61%), 822.1 (100%), 823.1 (47%), 824.1 (62%), 825.1 (27%), 826.1 (11%). Found: 816.1 (13%), 817.1 (7%), 818.1 (7%), 819.1 (34%), 820.1 (43%), 821.1 (66%), 822.1 (100%), 823.1 (49%), 824.1 (64%), 825.1 (26%), 826.1 (13%).

[cis-Di(thiocyanato)-({4,4′-dicarboxy}-2,2′-bipyridyl)-(4,4′-bis-{[3,5-bis(4-{2-ethylhexloxy}phenyl)-(E)-styryl}-2,2′-bipyridine)]ruthenium(II) ***11***. {RuCl(*p*-cymene)}$_2$ (50 mg, 0.08 mmol) and **5** (192 mg, 0.16 mmol) were dissolved in distilled *N*,*N*′-dimethylformamide (25 mL). The reaction mixture was heated at 80 °C under nitrogen for 4 h and then 2,2′-bipyridine-4,4′-dicarboxylic acid

(17) Garelli, N.; Pierre Vierling, P. *J. Org. Chem.* **1992**, *57*, 3046–3051.

(40 mg, 0.16 mmol) was added and the reaction mixture was heated at 150−160 °C for another 4 h in the dark to avoid isomerization. An excess of ammonium isothiocyanate (310 mg, 4.08 mmol) was added to the mixture, which was heated at 150 °C for a further 4 h. The reaction mixture was cooled to room temperature and the solvent was removed. Water (20 mL) was added, and the insoluble solid was collected by filtration and washed with distilled water (2 × 100 mL). The crude complex was dissolved in a solution of tetra-*n*-butylammonium hydroxide in methanol (5 mL). The concentrated solution was purified by column chromatography using Sephadex LH-20 with methanol as eluent. The main band was collected and solution concentrated. Addition of nitric acid (0.1 M, 10 mL) caused a precipitate to form, which was filtered. The residue was dissolved in methanol and precipitated with nitric acid (0.1 M, 10 mL) a further two times. The residue was finally washed with distilled water and dried to give **11** as a black solid (170 mg, 63%). Mp > 335 °C. Anal. Calcd for $C_{96}H_{108}N_6O_8RuS_2$: C, 70.3; H, 6.6; N, 5.1. Found: C, 70.4; H, 6.6; N, 5.1. λ_{max}(*N*,*N*′-dimethylformamide) 546 [log ε (dm^3 mol^{-1} cm^{-1}) (4.26)], 414 (4.29), 343sh (4.64). ν_{max} 3500 (br) (−OH), 2100 (−CN), 1719 (−C═O) cm^{-1}. δ_H (500 MHz, DMSO-d at 373K) 9.55 (1 H, d, *J* = 5.5, bipyH), 9.26 (1 H, d, *J* = 5.5, bipyH), 9.04 (1 H, bs, bipyH), 8.95 (1 H, bs, bipyH), 8.89 (1 H, bs, bipyH), 8.80 (1 H, bs, bipyH), 8.26 (1 H, d, *J* = 4.5, bipyH), 8.12 (1 H, d, *J* = 4.5, bipyH), 8.06 (1 H, d, *J* = 16, vinylH), 7.91 (4 H, m, G1-bpH), 7.86−7.64 (14 H, m, G1-bpH, vinylH, spH, bipyH), 7.48 (1 H, d, *J* = 5, bipyH), 7.43 (1 H, d, *J* = 16.5, vinylH), 7.38 (1 H, d, *J* = 5, bipyH), 7.10 (4 H, 1/2AA′BB′, spH), 7.05 (4 H, 1/2AA′BB′, spH), 3.99−3.93 (8 H, m, OCH_2), 1.79−1.69 (4 H, m, CH), 1.57−1.29 (32 H, m, CH_2), 0.99−0.87 (24 H, m, CH_3). *m*/*z* [MADI-TOF] Anal. Calcd. for $C_{96}H_{108}N_6O_8RuS_2$: 1632.7 (10%), 1633.7 (11%), 1634.7(10%), 1635.7 (28%), 1636.7(47%), 1637.7 (65%), 1638.7 (100%), 1639.7 (83%), 1640.7 (78%), 1641.7 (54%), 1642.7 (29%), 1643.7 (13%), 1644.8 (4%). Found: 1632.7 (8%), 1633.7 (11%), 1634.7(8%), 1635.7 (21%), 1636.7(58%), 1637.7 (67%), 1638.7 (100%), 1639.7 (88%), 1640.7 (80%), 1641.7 (52%), 1642.7 (41%), 1643.7 (12%), 1644.8 (10%).

[cis-Di(thiocyanato)-({4,4′-dicarboxy}-2,2′-bipyridyl)-(4,4′-bis{[3,5-bis(3,4-di{2-ethylhexloxy}phenyl)-(E)-styryl}-2,2′-bipyridine)]ruthenium(II) ***12***. {RuCl(*p*-cymene)}$_2$ (50 mg, 0.08 mmol) and **7** (276 mg, 0.16 mmol) were dissolved in distilled *N*,*N*′-dimethylformamide (30 mL). The reaction mixture was heated at 80 °C under nitrogen for 4 h; 2,2′-bipyridine-4,4′-dicarboxylic acid (40 mg, 0.16 mmol) was then added and the reaction mixture was heated at 150−160 °C for another 4 h in the dark to avoid isomerization. An excess of ammonium isothiocyanate (310 mg, 4.08 mmol) was added to the mixture, which was heated at 150 °C for a further 4 h. The reaction mixture was cooled to room temperature and the solvent was removed. Water (20 mL) was added and the insoluble solid was collected by filtration, and washed with distilled water (2 × 100 mL). The crude complex was dissolved in a solution of tetra-*n*-butylammonium hydroxide in methanol (5 mL). The concentrated solution was purified by column chromatography using Sephadex LH-20 with methanol as eluent. The main band was collected and solution concentrated. Addition of nitric acid (0.1 M, 10 mL) caused a precipitate to form, which was filtered off. The residue was dissolved in dimethylsulfoxide (10 mL) and then nitric acid (0.1 M, 10 mL) was added. The precipitate was collected at the filter, washed with distilled water and dried to give **12** as a black solid (190 mg, 54%). Mp > 335 °C. Anal. Calcd for $C_{128}H_{172}N_6O_{12}RuS_2$: C, 71.4; H, 8.1; N, 3.9. Found: C, 71.5; H, 8.05; N, 3.8. λ_{max}(*N*,*N*′-dimethylformamide) 545 [log ε (dm^3 mol^{-1} cm^{-1}) (4.28)], 415 (4.29), 338sh (4.66). ν_{max} 3500 (br) (−OH), 2100 (−CN), 1726 (−C═O) cm^{-1}. δ_H (500 MHz, DMSO-d, 373K) 9.55 (1 H, d, *J* = 5.5, bipyH), 9.28 (1 H, d, 1H, *J* = 6, bipyH), 9.06 (1 H, bs, bipyH), 8.97 (1 H, bs, bipyH), 8.91 (1 H, bs, bipyH), 8.81 (1 H, bs, bipyH), 8.29 (1 H, d, *J* = 5, bipyH), 8.16 (1 H, d, *J* = 5, bipyH), 8.04 (1 H, d, *J* = 16.5, vinylH), 7.92 (2 H, m, G1-bpH), 7.84−7.64 (8 H, m, G1-bpH, vinlyH, bipyH), 7.52−7.25 (11 H, m, vinylH, bipyH, spH), 7.10 (2 H, 1/2AA'BB', spH), 7.06 (2 H, 1/2AA′BB′, spH), 4.06−3.92 (16 H, m, OCH_2), 1.78−1.66 (8 H, m, CH), 1.58−1.27 (64 H, m, CH_2), 0.99−0.83 (48 H, bm, CH_3). *m*/*z* [MADI-TOF] Anal. Calcd for $C_{128}H_{172}N_6O_{12}RuS_2$: 2145.2 (7%), 2146.2 (10%), 2147.2 (11%), 2148.2 (24%), 2149.2 (43%), 2150.2 (65%), 2151.2 (100%), 2152.2 (99%), 2153.2 (92%), 2154.2 (71%), 2155.2 (43%), 2156. Two (22%), 2157.2 (10%). Found: 2145.2 (7%), 2146.1 (12%), 2147.2 (11%), 2148.1 (18%), 2149.1 (44%), 2150.1 (57%), 2151.1 (100%), 2152.1 (99%), 2153.1 (83%), 2154.1 (60%), 2155.1 (39%), 2156.1 (18%), 2157.1 (11%).

[cis-Di(thiocyanato)-({4,4′-dicarboxy}-2,2′-bipyridyl)-(4,4′-bis-{[3,5-bis(3,4,5-tri{2-ethylhexloxy}phenyl)-(E)-styryl}-2,2′-bipyridine)]ruthenium(II) ***13***. {RuCl(*p*-cymene)}$_2$ (40 mg, 0.06 mmol) and **9** (287 mg, 0.13 mmol) were dissolved in distilled *N*,*N*′-dimethylformamide (25 mL). The reaction mixture was heated at 80 °C under nitrogen for 4 h and then 2,2′-bipyridine-4,4′-dicarboxylic acid (32 mg, 0.13 mmol) was added and the reaction mixture was heated at 150−160 °C for another 4 h in the dark to avoid isomerization. An excess of ammonium isothiocyanate (250 mg, 3.26 mmol) was added to the mixture, which was heated at 150 °C for a further 4 h. The reaction mixture was cooled to room temperature and the solvent was removed. Water (20 mL) was added, and the insoluble solid was collected by filtration and washed with distilled water (2 × 100 mL). The crude complex was dissolved in a solution of tetra-*n*-butylammonium hydroxide in methanol (5 mL). The concentrated solution was purified by column chromatography using Sephadex LH-20 with methanol as eluent. The main band was collected and solution concentrated. Addition of nitric acid (0.1 M, 10 mL) caused a precipitate to form, which was filtered off. The residue was dissolved in dimethylsulfoxide (10 mL) and then nitric acid (0.1 M, 10 mL) was added. The precipitate was collected at the filter, washed with distilled water and dried to give **13** as a black solid (105 mg, 30%). Mp > 335 °C. Anal. Calcd for $C_{160}H_{236}N_6O_{16}RuS_2$: C, 72.1; H, 8.9; N, 3.15. Found: C, 72.1; H, 8.9; N, 3.2. λ_{max}(*N*,*N*′-dimethylformamide) 545 [log ε (dm^3 mol^{-1} cm^{-1}) (4.31)], 416 (4.30), 337sh (4.66). ν_{max} 3500 (br) (−OH), 2100 (−CN), 1726 (−-C═O) cm^{-1}. δ_H (500 MHz, DMSO-d, 373K) 9.56 (1 H, d, *J* = 5, bipyH), 9.29 (1 H, d, *J* = 5.5, bipyH), 9.06 (1, H, bs, bipyH), 8.96 (1 H, bs, bipyH), 8.91 (1 H, bs, bipyH), 8.81 (1 H, bs, bipyH), 8.30 (1 H, d, 1H, *J* = 5, bipyH), 8.15 (1 H, d, *J* = 5.5, bipyH), 8.04 (1 H, d, 1H, *J* = 16, vinylH), 7.95 (3 H, m, G1-bpH), 7.84−7.74 (5 H, m, G1-bpH, vinylH), 7.71 (2 H, m, bipyH), 7.51 (1 H, d, *J* = 6, bipyH), 7.45−7.38 (2 H, m, vinylH and bipyH), 7.03 (4 H, s, spH), 6.96 (4 H, s, spH), 4.05−3.94 (16 H, m, OCH_2), 3.91−3.83 (8 H, m, OCH_2), 1.78−1.64 (12 H, m, CH), 1.60−1.25 (96 H, m, CH_2), 0.98−0.82 (72 H, m, CH_3). *m*/*z* [MADI-TOF] Anal. Calcd for $C_{160}H_{236}N_6O_{16}RuS_2$: 2657.7 (6%), 2658.6 (10%), 2659.7 (11%), 2660.7 (21%), 2661.6 (38%), 2662.6 (60%), 2663.6 (92%), 2664.6 (100%), 2665.6 (96%), 2666.6 (79%), 2667.6 (56%), 2668.6 (31%), 2669.6 (15%). Found: 2657.7 (4%), 2658.6 (7%), 2659.7 (8%), 2660.7 (19%), 2661.6 (28%), 2662.6 (58%), 2663.6 (94%), 2664.6 (100%), 2665.6 (90%), 2666.6 (75%), 2667.6 (43%), 2668.6 (29%), 2669.6 (15%).

Acknowledgment. This work was funded by the Australian Research Council (PLB Federation Fellowship), the Queensland State Government (PM Smart State Senior Fellowship), the Australian Department of Science, Education and Training (International Science Linkage scheme − International Consortium for Organic Solar Cells), the University of Queensland (Strategic Initiative − Centre for Organic Photonics & Electronics), and the Korea Research Foundation Grant funded by the Korean Government (MOEHRD) (KRF-2005-214-D00268).